

A Structural Health Monitoring Software Tool for Optimization, Diagnostics and Prognostics

Seth S. Kessler¹, Eric B. Flynn², Christopher T. Dunn³ and Michael D. Todd⁴

^{1,2,3}*Metis Design Corporation, Cambridge, MA, 02141, USA*

skessler@metisdesign.com

eflynn@metisdesign.com

cdunn@metisdesign.com

⁴*University of California San Diego*

mtodd@ucsd.edu

ABSTRACT

Development of robust structural health monitoring (SHM) sensors and hardware alone is not sufficient to achieve desired benefits such as improved asset availability and reduced sustainment costs. For SHM systems to be practically deployed as part of an integrated system health management (ISHM), tools must be created for SHM life-cycle management (LCM). To that end, SHM-LCM software has been developed to expedite the adoption of SHM into ISHM. The SHM-LCM software is a flexible application intended to manage the cradle-to-grave life-cycle of an SHM system for generic applications. There are 4 core modules to facilitate critical roles: Optimization, Calibration, Visualization, and Action. The Optimization module seeks to devise optimal sensor placement and excitation parameters in order to achieve probability of detection (POD) coverage requirements. The Calibration module is designed to guide a user through a series of material level tests in order to customize algorithm variables to the system being designed. The Visualization module is dedicated to generating a diagnostic composite picture based on data downloaded from the diagnostic server, which is "stitched" to the original 3D mesh, providing users with a manipulatable GUI to toggle between probability of damage distributions for various calibrated damage modes. Finally, The Action module generates residual performance plots (ultimate load or deflection for example) as a function of probability of damage, so detection confidence can be weighed against impact to the vehicle's capabilities. SHM-LCM software will enable SHM systems to be incorporated into ISHM by engineers rather than experts, making the technology more accessible, and commercially practical.

1. INTRODUCTION

Currently successful laboratory non-destructive testing and monitoring methods are impractical for service inspection of large-area structures due to the size and complexity of the support equipment required, as well as the time and cost associated with component tear-down. It is clear that new approaches for inspection are necessary. Structural Health Monitoring (SHM) denotes the ability to detect and interpret adverse "changes" in a structure to direct actions that reduce life-cycle costs and improve reliability. Essentially, minimally-invasive detection sensors are integrated into a structure to continuously collect data that are mined for information relating to damage such as cracks or corrosion. SHM is receiving increasing attention, particularly from the DoD community, to eliminate scheduled and/or manual inspections in lieu of condition-based maintenance for more efficient design practices and more accurate repair and replacement decisions. This methodology shift will result in significant savings in overall cost of ownership of a vehicle, as well as significant gains in operational safety.

For SHM to be successfully implemented, accurate diagnostic and prognostic models are essential. Not only do sensors need to be properly integrated to collect data, but diagnostic characterization of the health of the structure needs to be extracted and presented to the operator and/or maintainer in a timely and meaningful manner. Furthermore, the diagnostic information should be converted to prognostic predictions so that proper action regarding remaining useful life or necessary repair can be taken. There are presently limited methods for visualizing diagnostic data, mainly 2-D representations, and no proven software to explicitly link diagnostic and prognostic information. Some methods have been demonstrated for health & usage monitoring system (HUMS); however, these systems provide far less detailed information compared to what is expected from an SHM system.

Kessler et al. This is an open-access article distributed under the terms of the Creative Commons Attribution 3.0 United States License, which permits unrestricted use, distribution, and reproduction in any medium, provided the original author and source are credited.

The overall approach taken by the current investigators was a system optimization problem; attempting to maximize detection capabilities with minimal impact to the test structure and at minimal cost, both capitalized and risk-generated. Hundreds of sensors densely spaced over a test structure would certainly have the best opportunity to precisely resolve damage locations, but this would obviously be impractical for real-life applications due to the quantity of instrumentation required (cables, data acquisition hardware, etc) or other incurred penalties (e.g. weight on an aircraft). Therefore the chosen approach was to use Bayesian risk function to assign costs to missed-damage, false-positives, and localization error as well as associating a cost with each sensor (where cost here is not monetary necessarily, but a relative metric for comparing the value of each parameter).

The actual physical SHM sensors and hardware considered for this work were part of the MD7 digital SHM system. This includes the IntelliConnector™ distributed digitization hardware, the VectorLocator™ analog sensing element and the HubTouch™ data accumulator. This system efficiently facilitates piezoelectric-based detection by allowing serial connections between sensors to minimize cabling, and by using a pulse-echo mode (same node sends and received the guided wave) the sensors can be spaced much further apart as compared to pitch-catch methods (where one element senses and another remote element receives the response). In particular, the VectorLocator provides not only amplitude information, but also phase using 6 local PZT sensing elements, thus being able to support both coherent and incoherent-based algorithms.

The algorithms used were a hybrid collection of functions making use of both coherent and incoherent information in the data. Data for each sensor is processed separately, then ultimately summed in a weighted fashion across the test structure. Further logic is also deployed to eliminate anomalies and invalid features. Generally, this process is analogous to active sonar. Damage ("targets") are detected and/or localized by generating ultrasonic elastic waves and watching how they bounce off of potential targets. Because a test structure is arguably far more complex than the open ocean, producing potentially far more "false targets" (such as boundaries, stiffeners, rivets, size changes, material interfaces, etc.), this approach takes advantage of embedding probabilistic models into the wave propagation/scattering process so that likelihood-based judgments can be made about the damage targets. These judgments may be understood in appropriate performance terms—probability of detection, probability of localization, etc.—which directly supports the uncertainty quantification needed for decision-making.

Finally, the decomposed data must be displayed in a meaningful matter. Work was done to deploy a graphical-user-interface (GUI) that would allow 3D structures to be

represented with damage predictions stitched-in. Controls are deliberately included to allow knowledgeable users to deviate from default algorithm and display parameter values to refine the image or search for smaller damage that is obfuscated by severe damage locations. The software is also built in such a way so that diagnostic results can be exported to commercial finite element tools to provide prognostic information such as residual strength or stiffness.

A major advantage of this overall approach is its power to serve also as a design tool. Through the overarching probabilistic framework, if a client-defined objective is established for a given application (e.g., "must detect fatigue cracks < 1 mm oriented at any random angle with a probability of 95% and use no more than 1 sensor per square meter"), this approach allows for an a priori optimization of the sensor architecture before in-situ deployment to meet those objective(s). This provides tremendous potential cost savings, eliminating the "black box" and "trial and error" approaches to doing SHM system design.

2. SHM SYSTEM SENSORS AND HARDWARE

To achieve the overall goals of efficient damage detection, This research leverages hardware previously developed by the investigators, including distributed digitization hardware (MD7 IntelliConnector™), piezoelectric-based damage-localization sensors (MD7 VectorLocator™), and a data accumulation hub (MD7 HubTouch™). Together these elements combine to form the MD7 digital SHM system.

2.1 MD7 IntelliConnector™

The IntelliConnector™ is a digital sensor infrastructure; a direct replacement of traditional instrumentation such as oscilloscopes and function generators. This device greatly reduces cable weight by allowing data to be carried over a serial sensor-bus and increases signal fidelity by digitizing at the point-of-measurement to eliminate EMI. Hardware requirements are also minimized through distributed local processing. The IntelliConnectors™ excite analog sensors mated through micro-connectors and digitize their response. Individual nodes are connected in a single daisy-chained serial sensor bus using flat-flexible-cable (FFC).

2.2 MD7 VectorLocator™

A patented method is used to determine relative phase information for the sensor responses, by surrounding a central actuating disk with multiple sensing disks, known as the VectorLocator™. The actuating and sensing component consists of seven piezoelectric wafers that are integrated into a custom flex-circuit assembly that connects to the IntelliConnectors™. These elements are permanently mounted on the structure being monitored. The closely spaced set of piezoelectric elements in each node form a phased array, which enables the identification of both range and bearing to multiple damage sites using a single node.

This is in contrast to isolated piezoelectric elements which can only identify range, necessitating the use of multiple spatially separated elements to localize damage sites through a triangulation process that has been shown to be susceptible to corruption by multiple damage sites. Also, if relative time of arrival at the sensor elements is used, a ray indicating angle to damage can be generated without any wavespeed information. Thus damage can be localized by simply finding the ray intersection of 2 of these vector-locator nodes. The VectorLocator™ method can be deployed actively using GW to determine the location of damage as described here, or passively in acoustic emission mode the same equations can be used to describe the position of an impact.

3. SENSOR PLACEMENT OPTIMIZATION

SHM systems are decision makers. At any given time, or according to any given measurement, the SHM system needs to be designed to let the operator know whether or not a potential problem in the structure requires action. As such, an SHM system will likely have to make hundreds or thousands of decisions while the structure is undamaged before a defect actually develops. During this time, it is important that the SHM system correctly decides that the structure is healthy as frequently as possible. If the SHM system constantly demands costly, unnecessary manual inspections then it provides no benefit to the monitored structure and its operation. It is important, then, that the design of SHM systems and the evaluation of their performance consider the total risk posed by all forms of decision errors.

3.1 Theory

The presently proposed approach to SHM is the minimization of the expect cost, or Bayes Risk, associated with an SHM system through the optimal design of detection algorithms and system hardware (i.e., sensor placement). Put simply, the Bayes Risk is sum of the costs of all possible detection outcomes (detection, missed detection, false alarm, etc) weighted by their probability of occurring. This can be represented as

$$R = \sum_{d,\theta} C(d,\theta)P(d|\theta,e)P(\theta) + C(e) \quad (1)$$

where d is the set of possible decisions the SHM system makes (e.g., in a binary decision case, “continue operation,” or “stop and inspect”), θ is the damage state of the structure, and e is the design of the SHM algorithms and hardware. The first probability term describes the statistical performance of the SHM detection system and the second probability term reflects the prior probabilities of damage, if known. The optimal SHM algorithm and hardware design is then defined as:

$$e^* = \arg \max_e R(e) \quad (2)$$

A key component of the proposed approach to structural health monitoring is the optimization of the placement of sensor nodes according to the minimization of the expect cost, or Bayes Risk, associated with the decisions made by the SHM system. The calculation of the Bayes Risk for an arbitrary set of node placements then requires accurate models of the wave propagation process and detector statistics parameterized by the node coordinates. To simplify the modeling, the structure is divided into discrete regions. Then to determine the total Bayes Risk of the structure, the localized Bayes Risk is calculated for each region and sum. The statistical performance of detectors for each region is evaluated with any given set of node placements using an analytical model of the wave propagation and scattering process. This model includes beam spread, line of site, directional scattering, and transmission across the doublers. According to this stochastic model, the detector described above, and an optimal set of detector thresholds, maps can be constructed of the expected localized detection and false alarm rates. Examples of these maps for a two-node arrangement are shown in Figure 1. Note the effect of line of site and the doublers in the two maps. Nodes were optimally placed in a greedy algorithm fashion. Starting with one node, one at a time, each node is added so that it optimally compliments the existing fixed arrangement. As such, there always exists a subset of n nodes from the total N nodes that is near-optimal. Near-optimal in this case means a guaranteed performance of at least:

$$U_{Greedy}[n] \geq \left(1 - \left(\frac{n-1}{n}\right)^n\right) U^*[n] > 0.63U^*[n] \quad (3)$$

where $U^*[n]$ is the performance (or utility) of the optimal arrangement of nodes.

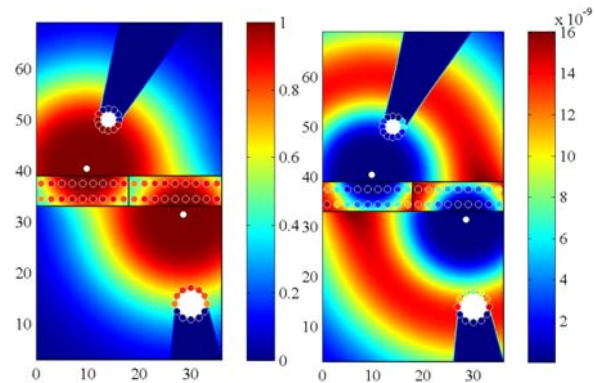


Figure 1: Local detection rates (left) and, false alarm rates (right) for a two-node arrangement. Nodes are indicated with small white-filled circles.

3.2 Optimization Example

A structure was divided into two sets of discrete regions. The first set forms a uniformly spaced grid covering the structure. The second set is assembled from the identified hot spots on the structure consisting of the localized area around each of the bolt holes. Each region from the uniform and hot-spot sets is then assigned a probability of damage. Wave scattering was modeled according to a 5 mm crack with uniform random orientation. Imaging noise was modeled as Raleigh distributed. Noise parameters were fitted from data acquired over two days from three-foot-square plate instrumented with identical nodes. The probabilities and error penalties were assigned as follows:

- Probability of damage being introduced: 80%
- Conditional probability of damage being introduced at hot spots: 60%
- Conditional probability of damage being introduced away from hot spots: 40%
- Penalty of missed detection / penalty of false alarm = 2/1

Figure 2 shows the optimized arrangement of six nodes on a map of the resulting normalized risk. The nodes are numbered in order of their placement by the greedy algorithm. The normalized risk for the greedy-chosen arrangement fell within 5% of the true optimal 6-node arrangement as found by an exhaustive genetic algorithm search. Figure 3 provides a graph of the normalized risk versus node count. When the cost of each additional node is added to the risk calculation, the risk versus node count will have a minimum that indicates the optimal number of sensors to use. Figure 3 demonstrates that adding additional nodes has diminishing returns when accounting for per-node costs.

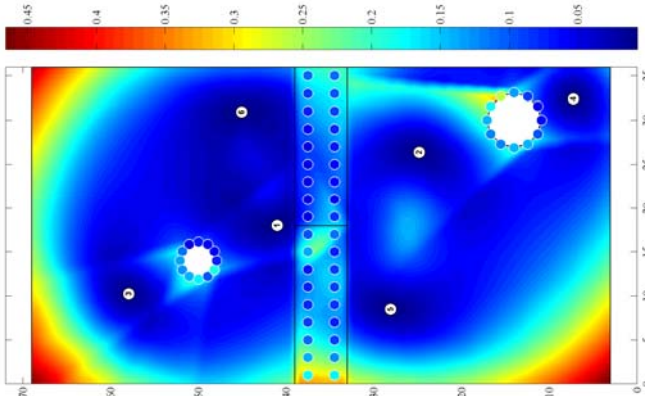


Figure 2: Optimal 6 node arrangement with map of normalized local risk

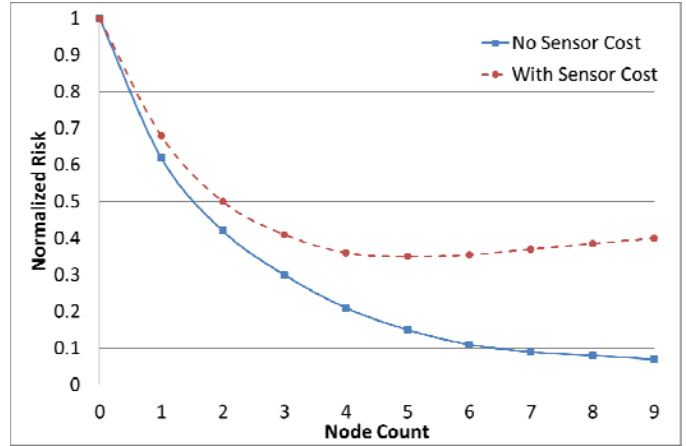


Figure 3: Normalized risk versus node count

4. DIAGNOSTIC ALGORITHMS

Active sensing involves mechanically exciting a structure and in turn measuring the response in order to gain information regarding the potential presence of damage. When one dimension of the structure being excited is relatively small compared to the other two, such as in a plate-like structure, and the wavelength(s) of excitation are of the same order as this dimension, the process is referred to as guided-wave active sensing.

The MD7 system works in an analogous fashion to active sonar. One at a time, each MD7 node actuates a series of narrow-band, ultrasonic mechanical pulses, or “pings”, using its central actuation transducer. These pulses propagate through the structure, reflect and scatter at geometric features, such as plate boundaries, as well as at potential damage, and are then sensed by the six sensing transducers on the node. The node digitizes the sensed responses and sends the data to the accumulation hub where it is stored for later retrieval and processing

The recorded responses are used to determine the range(s), bearing(s), and size(s) of potential damage in the structure relative to each node. In traditional active sonar applications, bearing is often determined in one of two ways. The first is to physically arrange the sonar array to maximize its sensitivity in one direction, and then mechanically orientate, or steer, the array to scan multiple directions. The second approach is to artificially introduce delays in the acquired, digitized responses in order to electronically steer the array through a processes known as beam forming. For the current application, the latter approach has two distinct advantages. First, the position of the array elements (i.e. sensing transducers) can be fixed so there are no moving parts. Second, a single actuated pulse and sensed response can be used to simultaneously scan for damage in every direction. This directional scanning through electronic steering forms the basis of the present approach to ultrasonic guided wave imaging.

4.1 Beamforming

Optimal detectors can be derived according to statistical likelihood tests on the measured responses for the presence and location of damage. Depending upon the specific objective(s), such detectors provide a means of combining measurement data to build a set of test statistics $T(x)$ (sometimes referred to as “damage features”) that can be compared to a threshold (determined by a risk analysis) in order to make decisions regarding the existence and/or location of damage on the structure. In most cases, where localization is of prime importance, the time of flight from the actuator to the potentially damaged region to the sensor for a given wave number can be reasonably estimated based on an average group velocity computed from the (likely heterogeneous) material and geometric properties along the propagation path. With this in mind, a common localization detection approach for each region in a structure is one that delays and sums the measurements from the different transducer pairs so that they will additively combine at the true location of damage, resulting in an “image” of highly constructive scatter relative to the background noise. However, the relative average phase velocities from each transducer pair to each region of the structure can be more difficult to predict. This leads to two basic forms of detectors based on the statistical model of the measurements: coherent and incoherent beam forming.

In the case where the relative phase velocity is different and unknown between transducer pairs, the envelopes of the waveforms must be summed together in order to eliminate the dependence on phase. Otherwise, the delayed and summed waveforms run the risk of destructively interfering at the true location of damage and/or constructively interfering away from damage. If we represent the baseline-subtracted acquired waveform from each transducer pair on node n according to its complex analytic signal w_{nm} , then the test statistic for the incoherent (“phase ignorant”) detector for damage at \mathbf{x} reduces to

$$T_I(\mathbf{x}) = \sum_{m=1}^M |w_m(t - \tau(m, \mathbf{x}))| \quad (4)$$

where $\tau(m, \mathbf{x})$ is time of flight from transducer pair m to \mathbf{x} .

In the case where the relative phase velocity between transducer pairs is the same, the delayed waveforms can be combined coherently, without enveloping, which is referred to as coherent beamforming. The test statistic for the coherent detector can then be expressed as:

$$T_C(\mathbf{x}) = \left| \sum_{m=1}^M w_m(t - \tau(m, \mathbf{x})) \right| \quad (5)$$

where the magnitude is taken after summation rather than before. Coherent beamforming is ideal since the summation of the delayed waves tend to destructively combine at all

locations except the true location of damage. However, in order for the average phase velocities along the path to each region of the structure to be the same, the transducers must be very closely spaced (less than a characteristic interrogation wavelength apart), limiting their coverage of the structure. In practice, for narrowband signals, the time delays are substituted by computationally faster phase shifts. As such, arrays of sensors that make use coherent beam forming, such as those packaged in each MD7 node, are referred to as phased arrays.

Each sensor node implemented by MDC involves a single actuating transducer surrounded by six sensing transducers. Across the transducers in each node, the average phase velocity along the path to any given region is approximately equal, allowing for coherent beamforming. From node to node, however, the average phase velocity is generally not equal and as such the scattered signals must be combined incoherently. This hybrid approach enables both effective imaging through coherent beam forming within each node as well as effective coverage of large areas through the placement of multiple nodes.

$$T_H(\mathbf{x}) = \left\| \sum_{n=1}^N \sum_{m=1}^6 w_{nm}(t - \tau(n, m, \mathbf{x})) \right\| \quad (6)$$

Figure 4 shows a graphical representation of the summation process. The scans on the left are the result of coherent summation of the individual sensing-transducers’ measurements with appropriate time delays while the image on the right shows the result of the incoherent summation of multiple MD7 nodes.

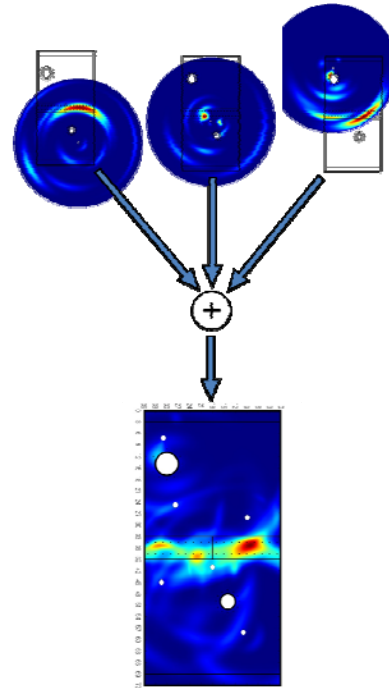


Figure 4: Summation of multiple single-node radial scans

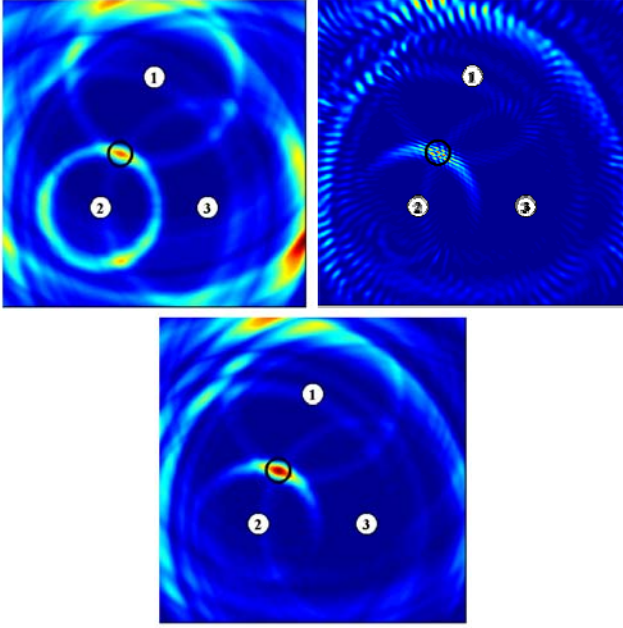


Figure 5: Incoherent (left) coherent (right) and hybrid (bottom) imaging using three nodes. The 0.25 inch disc magnet is located at the center of the open black circle.

Figure 5 shows a summary of results from these three imaging approaches for detecting a 0.25 inch magnet added to a three foot square plate. As shown, with coherent beamforming, a single node can identify both range and bearing of wave-scattering damage. Sensing systems that are not capable of coherent beamforming, such as sparse transducer arrays, can only identify range to a target, forcing them to rely on multiple, widely spaced, sensing elements in order to triangulate the damage location. This significantly reduces the necessary instrumentation footprint of the MD7 system when compared to traditional ultrasonic guided wave systems.

4.2 Matched Pursuits

One of primary and most unique aspects of the present data processing approach is the using of matching pursuit algorithms for identifying scatter targets. This is done by decomposing the 2D radial scans for each node into a sum of wave reflection packets, so that the scans can be approximated as

$$I^*(r, \theta) = \sum_n a_n K(r - r'_n, \theta - \theta'_n) \quad (7)$$

where a'_i , r'_i and θ'_i are the maximum likelihood estimates of the amplitude, range and bearing of the largest wave reflection and $K(r, \theta)$ is the wave reflection shape function. The wave reflection shape function depends on the shape and frequency of the excitation pulse as well as the layout of the sensing array within each node.

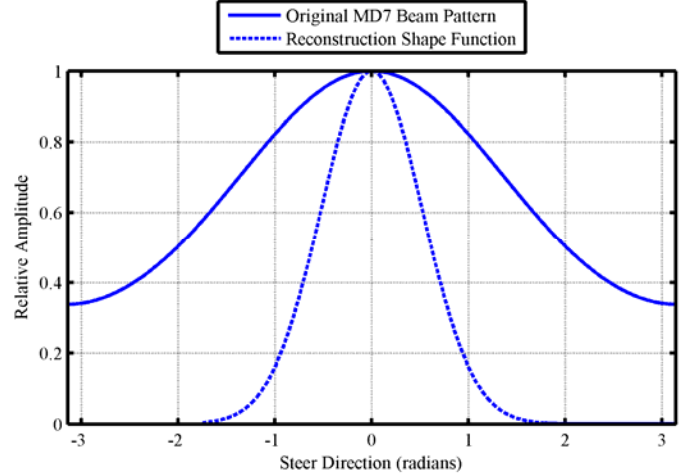


Figure 6: Beam pattern for 46 mm wavelength wave incident on the MD7 node

In the case of the MD7 node and the pulse width and frequency used in this test, the shape function can be expressed as

$$K(r, \theta) = \exp\left(\frac{-r^2}{2\sigma_r^2}\right) B(\theta) \quad (8)$$

where σ_r^2 is the width of the excitation pulse and is the beam pattern for a wave incident at broadside (zero degrees). The beam pattern is graphed in Figure 6 (solid line) for the primary wavelength used in testing and the circular sensor configuration on the MD7 nodes. The function represents the leakage of a wave incident at zero degrees into other look directions in the radial scan.

The amplitudes, ranges, and bearings of the wave packets are estimated according to the following matching pursuit algorithm:

1. Identify range, bearing, and amplitude corresponding the global maximum of the radial scan image

$$\{r'_n, \theta'_n\} = \arg \max_{r, \theta} I(r, \theta), \quad a'_n = I(r'_n, \theta'_n) \quad (9)$$

2. Subtract the reconstructed wave packet from the radial scan image

$$I(r, \theta) = I(r, \theta) - a_n K(r - r'_n, \theta - \theta'_n) \quad (10)$$

3. Repeat until the error the between the original image and the reconstructed image reaches a minimum

$$N_{Optimal} = \arg \min_N \sum_{r, \theta} \left(I(r, \theta) - \sum_{n=1}^N a_n K(r - r'_n, \theta - \theta'_n) \right)^2 \quad (11)$$

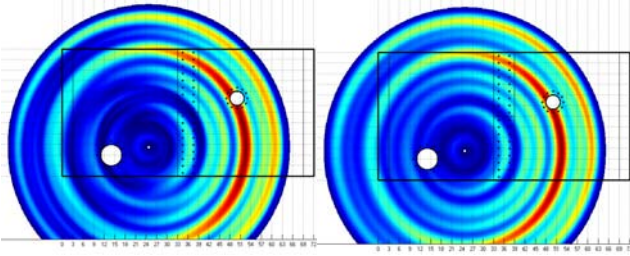


Figure 7: Original radial scan for single MD7 node (left) and reconstructed scan (right) using reflection packets estimated using matching pursuit algorithm

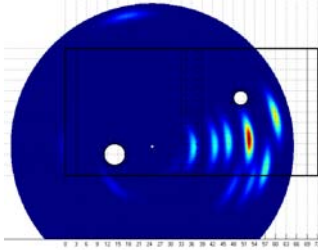


Figure 8: Reconstructed scan using narrowed-angle reflection shape function

Figure 7 shows the original radial scan for a single MD7 node (top) and a reconstructed image using discrete reflection packets. As can be seen in the figure, the natural wave reflection shape functions leave a large degree of ambiguity in the target bearing. When the responses from multiple nodes are combined, this can lead to significant error in the target localization. To remedy this, the imaging software alternatively reconstructs the images using the same estimated target amplitudes, ranges, and bearings, but with a narrower shape function, as depicted in Figure 6 (broken line). Figure 8 shows the same reconstructed radial scan image using the narrower shape function. Here, the precise locations of the potential reflection targets can be more readily identified.

5. PATH TO PROGNOSTICS

The development of sensors, hardware and diagnostic algorithms alone is not sufficient to achieve desired benefits for SHM. At best, current SHM systems can provide diagnostic information—typically in a proprietary and/or stand-alone format—and furthermore require a team of subject-matter experts to properly devise an installation strategy, calibrate algorithms and interpret the data. It is evident that for SHM system to be practically deployed as part of an integrated system health management (ISHM), tools must be created for SHM life-cycle management (LCM). To that end, SHM-LCM software has been developed to manage the cradle-to-grave life-cycle of an SHM system for generic applications. The initial version focuses on the MD7 pulse-echo style guided-wave SHM sensors previously described; however, the intent is to develop a framework that could eventually be sensor

agnostic. There are 4 core modules to facilitate critical roles: Optimization, Calibration, Visualization, and Action.

The Optimization module seeks to devise optimal sensor placement (using the Bayesian principals previously described) and excitation parameters in order to achieve probability of detection (POD) coverage requirements. This module is fueled by a 3D mesh of the structure to be monitored, and allows a user to impose POD distribution through a graphical user interface (GUI), resulting in a list of grid point to locate SHM sensors to meet these requirements.

The Calibration module is designed to guide a user through a series of material level tests in order to customize diagnostic algorithm variables (using the hybrid beamforming approach as previously described) to the system being designed. The output would be a file to be uploaded onto the SHM system diagnostic server (could be a local data accumulator or remote slot-card in a HUMS or AHM system box) that would take individual sensor raw data, translate it to diagnostic results, and fuse data from both active and passive sensor sources to compile a complete diagnostic picture including both structural and sensor health with quantified uncertainty.

5.1 Visualization Software

The Visualization module is dedicated to generating a diagnostic composite picture based on data downloaded from the diagnostic server. A prototype of the visualization tool was developed to help present ultrasonic imaging data to the user, seen in Figure 9. The idea is that the input to the software would be a) finite element mesh from a designer, and b) probability distribution as a function of damage size from diagnostics algorithms. The software would then stitch these results to the mesh and allow 3D visualization and manipulation (zoom, rotate, etc) of the diagnostic results on the actual geometry. Controls in the form of “sliders” are provided to the user to be able to control key algorithms variables, as well as adjust the upper and lower visualization thresholds. The intention is that eventually users will be able to toggle between probability of damage distributions for various calibrated damage modes within the GUI as well, as separated using time-windowed pattern recognition techniques such as K nearest neighbor (KNN).

This all contributes to providing a system that “feels” more like conventional NDE, where, while there are default settings, a knowledgeable/advanced user could refine the results for a more precise location, or alternatively find smaller damage that is hidden by the effects of large damage response. A screen-shot of the full three dimensional visualization of the software is shown in Figure 10.

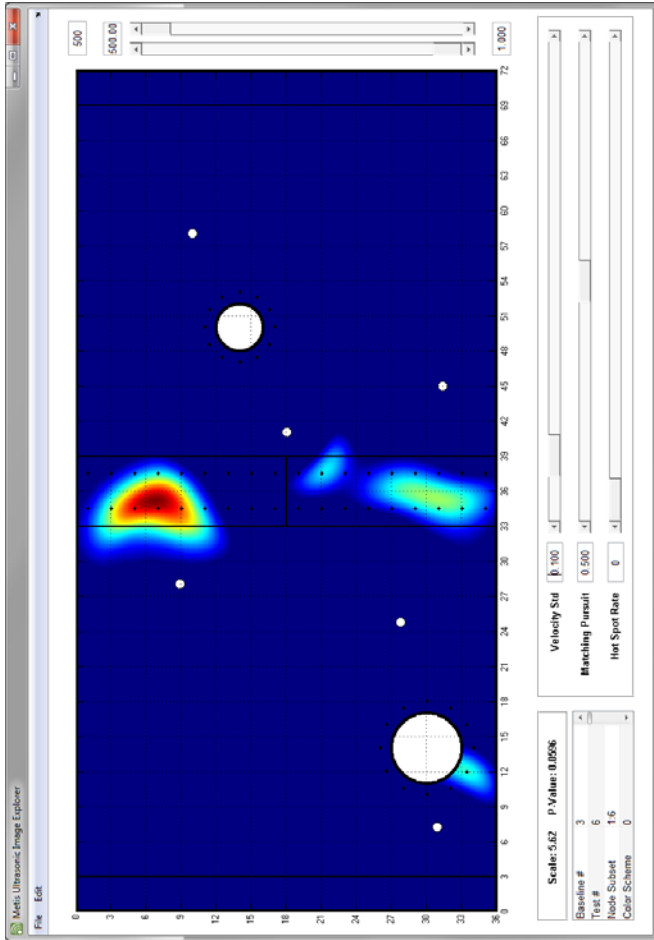


Figure 9: Prototype diagnostic visualization software (2D)

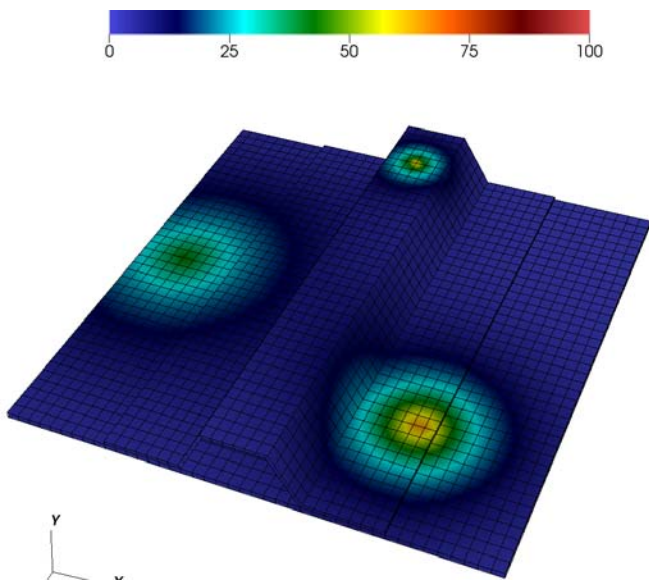


Figure 10: Prototype diagnostic visualization software (3D)

5.2 Residual Performance

The final Action module completes the life-cycle management by providing users with guides for responses to the diagnostic results. This includes the generation of residual performance plots (ultimate load or deflection for example) as a function of probability of damage, using an embedded finite element engine that compares baseline models to those with reduced material properties or un-tied coincident nodes. Using this module, users can weigh detection confidence against the impact to the vehicle's capabilities; and eventually this type of methodology could be embedded for real-time usage to enable fly-by-feel methodologies. Finally, repair optimization tools are planned to be incorporated in order to suggest means of restoring original performance for an assumed damage confidence-level design point.

6. CONCLUSION

This paper presents the framework of a software tool being developed to manage the life-cycle for SHM systems. The core elements include optimization, calibration, visualization and action modules. Much of the present research has focused on the optimization piece, using a Bayesian risk minimization approach to determine optimal sensor placement to minimize false positives while providing the desired coverage, attempting to use the minimum number of sensors to convey efficiency. Furthermore work was performed with regards to diagnostic algorithm calibration using a hybrid beamforming method. Finally, a visualization approach was demonstrated with an intuitive and fast GUI for near-real time display of diagnostic results with NDE-like controls. Overall, while the proposed framework was demonstrated using pulse-echo style guided wave sensors, it was developed such that it will be able to become sensor agnostic, and also be able to easily link up with prognostic methods for evaluating residual performance. The SHM-LCM software will enable SHM systems to be incorporated into ISHM by engineers rather than experts, making the technology more accessible, and commercially practical.

ACKNOWLEDGEMENT

This work was sponsored by the Office of Naval Research, under contract N00014-10-M-0301, monitored by Dr. Ignacio Perez. The authors would like to additionally thank Dr. Liming Salvino, Dr. Roger Crane, Dr. Mark Seaver and Dr. Benjamin Grisso for their guidance during this program. Metis Design Corporation was the prime contractor under this STTR topic N10A-T042, and University of California San Diego was the subcontracted research institute.

REFERENCES

- Fasel T. R., Kennel M. B., M. D. Todd, E. H. Clayton, M. Stabb, and G. Park, (2009). "Damage State Evaluation of Experimental and Simulated Bolted Joints Using Chaotic Ultrasonic Waves," *Smart Structures and Systems*, vol 5(4), pp. 329-344.
- Fasel T. R., Todd M. D., Park G., and C. Farrar (2006), "Plate Damage Identification Using Up-converted Chaotic Excitations and Time-reversal Acoustics," *Proc. SPIE Smart Structures/NDE 6177*, San Diego, California, February 27-March 2.
- Fasel T. R. and M. D. Todd, (2010) "An Adhesive Bond State Classification Method for a Composite Skin-to-Spar Joint Using Chaotic Insonification," *Journal of Sound and Vibration*.
- Flynn E. and M. D. Todd (2010). "Optimal Placement of Piezoelectric Actuators and Sensors for Detecting Damage in Plate Structures," *Journal of Intelligent Material Structures and Systems*, vol. 21(2), pp. 265-274.
- Flynn E. and M. D. Todd, (2010) "A Bayesian Approach to Optimal Sensor Placement for Structural Health Monitoring with Application to Active Sensing," *Mechanical Systems and Signal Processing*.
- Holmes C, Drinkwater BW, Wilcox PD (2005). Post-processing of the full matrix of ultrasonic transmit-receive array data for non-destructive evaluation. *NDT and E International*. vol. 38, pp.701-711.
- Kay SM (1998). *Fundamentals of Statistical signal processing, Volume 2: Detection theory*. Prentice Hall PTR.
- Kessler S.S. and P. Agrawal.(2007) "Application of Pattern Recognition for Damage Classification in Composite Laminates." *Proceedings of the 6th International Workshop on Structural Health Monitoring*, Stanford University
- Kessler S.S. and A. Raghavan (2008). "Vector-Based Localization for Damage Position Identification from a Single SHM Node." *Proceedings of the 1st International Workshop on Prognostics & Health Management*, Denver, CO
- Kessler S.S. and A. Raghavan (2009). "Vector-based Damage Localization for Anisotropic Composite Laminates." *Proceedings of the 7th International Workshop on Structural Health Monitoring*, Stanford University
- Mascarenas D., Todd M. D., Park G., and C. R. Farrar, (2007). "Development of an Impedance-Based Wireless Sensor Node for Structural Health Monitoring," *Smart Materials and Structures* vol 16(6), pp. 2137-2145.